

Second MaPhySto Workshop on

Inverse Problems

Inverse Problems from a Statistical Perspective
28-31 March 2001, Aalborg University, Denmark

Contents

1 Introduction	1
2 Content	1
3 Program	2
4 Abstracts (in alphabetical order)	4
5 List of speakers and participants	41

1 Introduction

This workshop was the second in a series organized by MaPhySto. The workshop brought together researchers with varied backgrounds, and common interest in inverse problems seen from a statistical perspective. There was a series of lectures by leading scientists having an active interest in the themes of the workshop. It fostered fruitful discussions on the role of statistics in solution of inverse problems.

The Workshop was organized by

- Martin B. Hansen (MaPhySto, Aalborg)
- Jens Ledet Jensen (MaPhySto, Aarhus)
- Steffen Lilholt Lauritzen (MaPhySto, Aalborg)

2 Content

The term inverse problems is used to denote a wide area of problems from both pure and applied mathematics, where one must recover information about a quantity or a phenomenon under study from measurements which are indirect and possibly noisy as well. This corresponds to the situations confronting engineers, scientists and industrial mathematicians on a daily basis. Informally, a direct problem corresponds to calculating the effect of some given cause, whereas the inverse problem corresponds to deriving the cause given some of its effects.

A practical example comes from the scattering of sound waves as occurs in ultrasonic imaging. The direct problem is to calculate the scattered waves given the scattering medium. On the other hand, the inverse problem consists in determining the structure of the scattering medium, given the wave

source and measurements of the scattered waves. As noise and uncertainty is inevitable in most applications the focus of the workshop will be on statistical aspects of inverse problems.

3 Program

Wednesday 28 March

09.30 - 10.15 Registration/Coffee
10.15 - 10.30 Welcome by Martin B. Hansen

Chairman: Steffen L. Lauritzen

10.30 - 11.30 **Finbarr O'Sullivan:** Quantitative analysis of data from PET imaging studies
11.30 - 11.45 Break
11.45 - 12.45 **Philip B. Stark:** Inverse problems in helioseismology
12.45 - 14.00 Lunch

Chairman: Martin B. Hansen

14.00 - 15.00 **Viktor Benes:** On stereological unfolding problems
15.00 - 15.15 Coffee
15.15 - 16.15 **Markus Kiderlen:** Discrete inversion of the spherical cosine transform in stereology

Thursday 29 March

Chairman: Jesper Møller

09.00 - 10.00 **Geoff Nicholls:** Bayesian inversion of boundary value data
10.00 - 10.30 Coffee
10.30 - 11.30 **Henning Omre:** Bayesian inversion in reservoir characterization with complex forward models
11.30 - 11.45 Break
11.45 - 12.45 **Klaus Mosegaard:** Geophysical applications of MCMC: Bayesian calculations and MC-optimization with slow forward algorithms
12.45 - 14.00 Lunch

Chairman: Bob Anderssen

14.00 - 15.00 **Odd Kolbjørnsen:** Bayesian inversion of piecewise affine inverse problems
15.00 - 15.15 Coffee
15.15 - 15.45 **Marcela Hlawiczkoa:** Estimating fibre process anisotropy

Friday 30 March

Chairman: Geoff Nicholls

- 09.00 - 10.00 **Grace Wahba:** Combining observations with models: Penalized likelihood and related methods in numerical weather prediction
- 10.00 - 10.30 Coffee
- 10.30 - 11.30 **Douglas W. Nychka:** Posterior distributions for numerical weather forecasts
- 11.30 - 11.45 Break
- 11.45 - 12.45 **Robin Morris:** 3D surface reconstruction as Bayesian inference
- 12.45 - 14.00 Lunch

Chairman: Grace Wahba

- 14.00 - 15.00 **Maria D. Ruiz-Medina:** Inverse estimation of random fields: Regularization and approximation
- 15.00 - 15.15 Coffee
- 15.15 - 16.15 **Anne Vanhems:** Nonparametric study of differential equations and inverse problems
- 16.15 - 16.30 Break
- 16.30 - 17.30 Round table discussion
- 19.00 Conference Dinner

Saturday 31 March

Chairman: Douglas Nychka

- 09.00 - 10.00 **Bob Anderssen:** Recovering molecular information from the mixing of wheat-flour dough
- 10.00 - 10.30 Coffee
- 10.30 - 11.30 **Frits Ruymgaart:** Spectral methods for noisy integral equations
- 11.30 - 11.45 Break
- 11.45 - 12.45 **Per Christian Hansen:** Inverse acoustic problems: Sound source reconstruction
- 12.45 - 14.00 Lunch

4 Abstracts (in alphabetical order)

Recovering molecular information from the mixing of wheat-flour dough

Bob Anderssen (Bob.Anderssen@cmis.csiro.au)

CSIRO Mathematical and Information Sciences, Canberra, Australia

The study of the mixing of wheat-flour dough on recording mixers, such as the Farinograph and Mixograph, is central to issues related to the milling of hard and soft wheats, the mixing of the resulting flours with water and other ingredients and the baking of the resulting doughs, as well as the design of scientific and industrial mixers. It plays an even greater and more fundamental role in the breeding of new wheat varieties. It is this latter aspect that will be the focus of the talk, though related aspects of bread, cake, pasta and Danish pastry making will not be ignored. It is guaranteeing their quality that is the control back to which plant breeding must respond.

The overall goal of the talk is an examination of some of the recent statistics and mathematics involved with extracting molecular information from various types of cereal chemistry experiments. In particular, the talk will focus on the following four topics:

1. **The Measurement of the Hardness of Wheat.**

When a particular variety of wheat is milled, the resulting flour will have either a unimodal or a bimodal size distribution. This relates directly to how the wheat has fractured during the milling. Hard wheats give the unimodal distribution, because the breakage is along cell walls and across the cells rupturing the starch granules. Soft wheats give the bimodal because the breakage is across the cells and around the starch granules with virtually no rupturing of the granules. Under the same milling conditions, the particle size of the hard wheats tends to be larger than for the softs. This strong and definite phenotype has been shown to have an unambiguous genetic explanation, in terms of genes that express proteins that induce adhesion between the gluten polymers and the surface of the starch granules.

For cereal chemists, hardness characterizes wheats according to the way in which they fracture, when subjected to grinding or milling (cf. Simmonds (1989)). Consequently, the hardness classes 'hard' and 'soft' serve as the primary basis for the initial classification of hexaploid wheats. However, the expression of the hardness genes is greatly influenced by the environmental conditions prevailing during grain filling, and during conditioning prior to flour milling (Manley et al, 1995; Bechtel et al, 1996; Delwiche, 2000). Genetically, it has been confirmed (Morris et al (1999)) that major allelic differences are assignable to a single dominant gene (Hardness, Ha) on the short arm of the 5D chromosome, and that various minor genes play a not unimportant role.

Independently, it has been confirmed (Osborne et al. (2001)) that, among the various procedures available, the Single-Kernel Characterization System (i.e. the SKCS 4100 instrument) provides the most discrimination in the measurement of wheat hardness. The SKCS 4100 instrument, now marketed worldwide by Perten Instruments, was initially developed at the USDA Grain Marketing and Production Research Center in Manhattan, Kansas. The original motivation was the need for objectivity and reliability in the classification and grading of US wheats. Full details about the operation of the SKCS instrument can be found in Martin et al. (1993). Some interesting questions arise about how the data recorded on such instruments should be modelled.

2. **Estimating the Number of Active Genes in Endosperm Development.**

In the study of genes in plants (and animals), an important issue is the identification, classification and comparison of the different genes that are active in various parts of the plant being examined at key stages in its development and growth. Among other things, such information is crucial in identifying the genes which play multiple roles and why. For example, for the efficient breeding of new wheat varieties, there is a need to know which genes are controlling the different stages of the starch and protein synthesis in the seeds.

However, when isolating such active genes experimentally, one is confronted with a situation where the different active genes are present in proportion to their expression activity. Consequently, one has the problem of estimating the number of distinct classes in a population of many individuals when a random sample of the individuals is all that is observed.

The same problem arises in many other contexts, for example, finding the species richness of some family of plants or animals in a specified environment (Fisher et al. (1943)), and estimating the size of an author's vocabulary (Efron and Thisted (1976)). As the sampling progresses, one will identify many members from the plants, animals or words (or genes) that are common, and few or no members from those that are uncommon. Bunge and Fitzpartick (1993) review the general problem, and Hass and Stokes (1998) focus on the situation where the total population size is known. In a recent analysis of wheat endosperm EST data, Wood et al. (2001) have shown that the earlier estimators of Goodman (1949) are more appropriate than the popular jackknife estimators.

3. **Recovering Molecular Information from High Resolution Mixograms.** In a traditional examination of the rheology of a wheat-flour dough, one first mixes the dough to peak dough development, then performs a suitable rheological experiment on the dough, and finally, formulates a qualitative or a simple mathematical modelling to analyse and interpret the observed behaviour of the dough. However, in such situations, the dough is being treated separately from the process by which it has been manipulated and produced, as if it were not a 'living system' (Meisner and Hostettler (1994)). An alternative approach is to directly utilize the information in the measurements obtained from a recording mixer, such as a MixographTM. This allows one to monitor the changing behaviour of a dough during mixing. In this way, the rheology of the dough is simulated as a part of the overall modelling of the mixing, and the constitutive relationship, which defines the changing rheology of the dough, is encapsulated implicitly within the modelling. The first step in a project to examine the feasibility and merit of performing such a study of the 'elongate-rupture-relax' mixing action of a MixographTM has been performed (Anderssen et al. (1998)). Normally, this is done as two separate steps where the dough is first mixed and then a sample of it is tested in an extension tester. In essence, a mixogram is a record of a series of extension tests that result from the 'elongate-rupture-relax' action which a MixographTM performs on the dough. The significance of this fact has been discussed in the recent literature (Gras et al. (2000)). In particular, it has been established that the bandwidth of a mixogram measures the changing extensional viscosity of a dough as it is being mixed.

Consequently, the flow and deformation occurring within a dough can be viewed as a repetitive loading process consisting of a sequence of 'elongate-rupture-relax' events. Chemically and physically, the elongation relates to the nature of the protein unfolding and cross-linking which the extension of the dough induces, while the relaxation relates to the partial refolding of the proteins, which occurs after the rupture, until the start of the next extension. Because the unfolding and refolding will occur at different rates, partially in response to the intensity of the cross-linking being stimulated by the mixing, one is led naturally to the hypothesis that 'the behaviour of wheat-flour dough during mixing is hysteretic in nature'. There are various ways

in which information about this hysteretic behaviour can be recovered from high resolution mixograms, such as the determination of the partial Bauschinger plots of the changing stress-strain behaviour of the dough during mixing (Anderssen and Gras (2000)) and the application of incremental change analysis (rainflow counting) to the individual 'elongate-rupture-relax' events (Anderssen and Gras (2001)). The advantage of such methodologies is that they give one the opportunity to see to the molecular level of the changing rheology of a dough during mixing, which is important for plant breeding investigations and the optimization of industrial mixing.

4. Recovering the Relaxation Spectrum and Molecular Weight Distribution of Polymers.

A popular molecular characterization of polymers is their molecular weight distribution. There are various ways in which it is estimated. They range from direct experimental procedures like gel chromatography electrophoresis and flow field flow fractionation (flow-FFF), to indirect measurement procedures such as the utilization of rheological measurements and mixing rules. The direct procedures spawn many interesting statistical and mathematical questions, while the indirect pose challenging questions about the formulation, solution and interpretation of inverse problems in rheology. In particular, questions about the formulation of the mixing rules that relate estimates of the relaxation modulus of the polymer (determined via a relaxation spectrum recovery process) to the molecular weight distribution. For example, some interesting mathematics arises when characterizing the family of mixing rules for which the scaling of rheological parameters, in terms of the molecular weight distribution, remains invariant. Recently, Anderssen and Loy (2001) have established how integral mean value theorems can be utilized to assist with the characterization.

It one takes a practical and important subject, like the breeding of new varieties of wheat, one finds that it has a long and interesting history that involves much science, statistics and mathematics. Because of the work of William Farrer, Australia has a long and distinguished history as a breeder, grower and exporter of wheat. Through the work of CSIRO's Wheat Research Unit (subsequently, the Grain Quality Research Laboratory), it has also played a dominant role in the development of the cereal science of wheat.

Cereal science lived on the invention and success of the recording mixer in the early 1930's. It has been molecular biology that has forced it to become more quantitative!

Assorted Bibliography

- Anderssen B, de Hoog F and Hegland M (1998) A stable finite difference ansatz for higher order differentiation of non-exact data, *Bulletin of the Australian Mathematical Society* 58, 223-232.
- R. S. Anderssen, P. W. Gras and F. MacRitchie, *J.Cereal Sci.*, 1998, 27, 167
- R. S. Anderssen, P.W. Gras and F. MacRitchie, *Chem. in Aust.*, 1967, 64(8), 3
- R. S. Anderssen, I. G. Gotz, and K.-H. Hoffmann, *SIAM J. Appl. Math.*, 1998, 58, 703
- R. S. Anderssen, P. W. Gras and F. MacRitchie, 'Proceedings of the 6th International Gluten Workshop: Gluten '96', RACI, North Melbourne, VIC, 1990, p. 249
- R. S. Anderssen and R. J. Loy (2001) On the scaling of molecular weight distribution functionals, *J. Rheology* (revised)
- Bechtel D B, Wilson J D and Martin C R (1996). Determining endosperm texture of developing hard and soft red winter wheats dried by different methods using the single-kernel wheat characterization system. *Cereal Chemistry* 73, 567-570.

- M. Brokate, K. Dressler and P. Krejci (1996) Rainflow counting and energy dissipation for hysteresis models in elastoplasticity, *Eur. J. Mech., A/Solids and Phase Transitions* 15 (1996), 705-737.
- M. Brokate and J. Sprekels (1996) *Hysteresis and Phase Transitions*, Springer, New York, 1996.
- J. Bunge and M. Fitzpatrick (1993) Estimating the number of species: A review, *J. Amer. Stats. Assoc.* 88 (1993), 364-373.
- R. H. Buchholz, *The Mathematical Scientist*, 1990, 15, 7
- D. R. Causton and J. C. Venus (1981) *The Biometry of Plant Growth*, Edward Arnold, London, 1981.
- Delwiche S R (2000) Wheat endosperm compressive strength properties as affected by moisture. *Transactions ASAE* 43:365-373.
- B. Efron and R. Thisted (1976) Estimating the number of unseen species: How many words did Shakespeare know? *Biometrika* 63 (1976), 435-447.
- R. A. Fischer, A. S. Corbet and C. B. Williams (1943) The relation between the number of species and the number of individuals in a random sample of an animal population, *J. Animal Ecology* 12 (1943), 42-58.
- Gaines C S, Finney P F, Fleege L M and Andrews L C (1996) Predicting a hardness measurement using the single-kernel characterization system. *Cereal Chemistry* 73: 278-283.
- Giroux MJ, Morris CF (1998). Wheat grain hardness results from highly conserved mutations in the friabilin components puroindoline a and b. *Proc. Natl. Acad. Sci. USA* 95, 6262-6266.
- L. A. Goodman (1949) On the estimation of the number of classes in a population, *Ann. Math. Stats.* 20 (1949), 572-579.
- P. W. Gras, H. C. Carpenter and R. S. Anderssen, *J. Cereal Sci.*, 2000, 31, 1
- P. W. Gras and R. S. Anderssen, 'Proceedings of the 49th Annual RACI Cereal Chemistry Conference', 2000,
- P. W. Gras, F. MacRitchie and R. S. Anderssen, 'MODSIM 97, Proceedings of International Congress on Modelling and Simulation', Modelling and Simulation Society of Australia, ANU, Canberra, ACT, 1998, p. 512
- P. W. Gras, G. E. Hibberd and C. E. Walker, *Cereal Foods World*, 1990, 35, 572
- P. J. Haas and L. Stokes (1998) Estimating species richness using the jackknife procedure, *J. Amer. Stats. Assoc.* 93 (1998), 1475-1487.
- K. L. Laheru (1992) Development of a generalized failure criterion for viscoelastic materials, *J. Propulsion and Power* 8 (1992), 756-759.
- C. R. Martin, R. Rousser and D. L. Brabec (1993) Development of a single-kernel wheat characterization system, *Trans. ASAE* 36 (1993), 1399-1404.
- J. Meisner and J. Hostettler, *Rheol. Acta*, 1994, 33, 1
- Morris C F, DeMacon V L and Giroux M J (1999) Wheat grain hardness among chromosome 5D homozygous recombinant substitution lines using different methods of measurement. *Cereal Chemistry* 76, 249-254.
- L. E. Nielsen, 'Mechanical Properties of Polymers and Composites', Marcel Dekker, New York, 1974.
- Osborne B G, Jackson R and Delwiche S R (2001) Rapid prediction of wheat endosperm compressive strength properties using the Single-Kernel Characterization System. *Cereal Chemistry* (in

press)

Pomeranz, Y., Peterson, C.J., Mattern, P.J. (1985) Hardness of winter wheats grown under widely different climatic conditions. *Cereal Chemistry* 62, 463-467

M. Shogren, J. L. Steele and D. L. Brabec, 'Proceedings of the Internat. Wheat Quality Conf.', Grain Industry Alliance, Manhattan, Kansas, 1997, p. 105

D. H. Simmonds (1989) *Wheat and Wheat Quality in Australia*, CSIRO Australia (Printed by William Brooks, Queensland), 1989.

Sissons M J, Osborne B G, Hare R A, Sissons S A and Jackson R (2000) Application of the Single-Kernel Characterization System to durum wheat testing and quality prediction. *Cereal Chemistry* 77: 4-10.

Williams P C, Sobering D, Knight J and Psotka J (1998) Application of the Perten SKCS-4100 single kernel characterization system to predict kernel texture on the basis of Particle Size Index, *Cereal Foods World*, 43, 550.

J. T. Wood, R. I. Forrester, B. C. Clarke and R. S. Anderssen (2001) Estimating the number of genes active in organism development, (in preparation)

Inverse estimation of random fields: Regularization and approximation

Jose Miguel Angulo (jmangulo@ugr.es)

Department of Statistics & Operations Research, University of Granada, Spain

Maria Dolores Ruiz-Medina (mruiz@ugr.es)

Department of Statistics & Operations Research, University of Granada, Spain

The problem of least-squares linear estimation of an input random field from the observation of an output random field in a linear system is considered. Different approaches to statistical inversion are reviewed, for example, in De Villiers (1992). Miller and Willsky (1995) present a wavelet-based approximation to the problem for uniparameter processes under a fractal-type prior model (*multiscale* model class) for the input. In the case where the system is defined by a mean-square integral equation relating two second-order random fields, Angulo and Ruiz-Medina (1999) derive a discretization method in terms of wavelet-based orthogonal expansions, related by the system equation, of the random input and output. An extension of this approach to the spatio-temporal case is given in Ruiz-Medina and Angulo (1999).

In this paper, we study the least-squares linear inverse estimation problem in a fractional generalised framework, using the definition of generalised random functions on fractional Sobolev spaces. The consideration of appropriate spaces according to the second-order properties of the input and observation (output, possibly affected by additive noise) random fields leads, under suitable conditions, to the definition of a stable solution. In the ordinary case, the solution derived is found in a distribution space. Furthermore, this approach allows the treatment of systems defined in terms of improper random fields with positive singularity orders. Finally, the computation of the solution, in both the generalised and ordinary cases, is carried out by using orthogonal expansions of the random fields involved in terms of dual Riesz bases (see Angulo and Ruiz-Medina, 1998, 1999). In the case where these dual Riesz bases are constructed from orthonormal wavelet bases, the approach presented provides a *multiresolution-like* analysis to the problem.

Angulo, J.M. and Ruiz-Medina, M.D. (1998). A series expansion approach to the inverse problem. *J. Appl. Prob.* **35**, 371-382.

Angulo, J.M. and Ruiz-Medina, M.D. (1999). Multiresolution approximation to the stochastic inverse problem. *Adv. Appl. Prob.* **31**, 1039-1057.

De Villiers, G. (1992). Statistical inversion methods. In M. Bertero and E.R. Pike (eds.), *Inverse Problems in Scattering and Imaging*, 371–392. Adam Hilger.

Miller, E.L. and Willsky, A.S. (1995). A multiscale approach to sensor fusion and the solution of linear inverse problems. *Appl. Comput. Harmonic Anal.* **2**, 127-147.

Ruiz-Medina, M.D. and Angulo, J.M. (1999). Stochastic multiresolution approach to the inverse problem for image sequences. In K.V. Mardia, R.G. Aykroyd, and I.L. Dryden (eds.), *Proceedings in Spatial Temporal Modelling and its Applications*, 57–60. Leeds University Press.

On stereological unfolding problems

Viktor Benes (benesv@karlin.mff.cuni.cz)

Department of Probability and Statistics, Charles University, Praha, The Czech Republik

In this lecture recent results in an inverse problem concerning stereology of particle systems will be reviewed. First the technique of derivation of an integral equation describing the problem is shown in the multivariate case. Besides theoretical solution more attention is paid to the numerical solution. The statistical extreme value theory may enter in the problem to discuss stereology of extremes. Finally a practical application in materials research is demonstrated.

Inverse acoustic problems: Sound source reconstruction

Per Christian Hansen (pch@imm.dtu.dk)

Informatics and Mathematical Modelling, Technical University of Denmark

Andreas P. Schuhmacher and Jørgen Hald

Brüel & Kjær A/S, Denmark

Karsten Bo Rasmussen

Oticon A/S, Denmark

The goal of this work is to develop robust software for computing the unknown surface velocity distribution on a complex acoustic source from measured acoustic field data. Hence we are faced with an inverse source problem, which involves forming a transfer matrix relating the pressure at every field point to the normal component of the surface velocity. The forward modeling is done by means of a boundary element method (BEM) and the inverse problem is solved by means of Tikhonov regularization. A practical case using a car tyre demonstrates the capabilities of our regularization scheme.

Throughout we use complex notation for harmonic time variation, and j denotes the imaginary unit. Our forward modeling problem is based on a *double-layer formulation*, which relates the pressure p at an arbitrary point P in the exterior region Ω to the normal component v_n of the velocity of the surface S :

$$p(P) = \int_S \mu(Q) \frac{\partial}{\partial n_Q} \left(\frac{e^{-jkR}}{4\pi R} \right) dS(Q), \quad P \in \Omega. \quad (1)$$

Here Q is a point on the surface, R is the distance between P and Q , k is the acoustic wave number, and μ is a distribution of *acoustic dipoles* on the surface. In addition we need the following relation between μ and the velocity v_n :

$$-j\omega\rho v_n(P) = \int_S \mu(Q) \frac{\partial^2}{\partial n_P \partial n_Q} \left(\frac{e^{-jkR}}{4\pi R} \right) dS(Q), \quad P \in S, \quad (2)$$

where ω is the angular frequency and ρ is the fluid density.

Equations (1) and (2) are both discretized by means of a boundary element method with triangular linear elements for both the geometry and the acoustic variables on the surface. The resulting linear systems of equations take the form

$$\mathbf{p} = \mathbf{G}\boldsymbol{\mu} \quad \text{and} \quad -j\omega\rho\mathbf{B}\mathbf{v}_n = \mathbf{Q}\boldsymbol{\mu}, \quad (3)$$

in which \mathbf{p} is a vector with the measurements of the acoustic pressure, while $\boldsymbol{\mu}$ and \mathbf{v}_n are vectors with BEM nodal values of the dipole sources and the normal surface velocities, respectively. Moreover, \mathbf{G} and \mathbf{Q} are complex matrices arising from the BEM discretization of the surface integrals, and \mathbf{B} is real symmetric matrix that takes the BEM geometry into account; see [5] for details. Combining the two systems in (3) we obtain

$$\mathbf{p} = -j\omega\rho\mathbf{G}\mathbf{Q}^{-1}\mathbf{B}\mathbf{v}_n = \mathbf{H}\mathbf{v}_n \quad (4)$$

which is a discrete inverse problem (in the terminology of [3]) that relates the unknown normal surface velocity $\boldsymbol{\mu}$ to the measured acoustic pressure \mathbf{p} via the “transfer matrix” $\mathbf{H} = -j\omega\rho\mathbf{G}\mathbf{Q}^{-1}\mathbf{B}$.

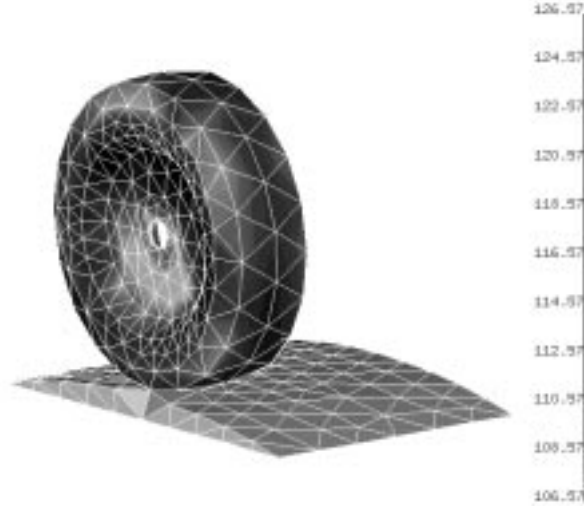


Figure 1: Reconstructed normal surface velocity v_n at 60Hz computed by means of the L-curve criterion.

We note that the above formulation breaks down for frequencies close to the so-called irregular frequencies (i.e., the eigenfrequencies of the associated interior problem), where the condition number of \mathbf{Q} becomes very large. An alternative formulation that can be used at these frequencies is described in [5].

The discrete inverse problem (4) is solved by means of Tikhonov regularization in the form

$$\min \left\{ \|\mathbf{H}\mathbf{v}_n - \mathbf{p}\|_2^2 + \lambda^2 \|\mathbf{L}\mathbf{v}_n\|_2^2 \right\} \quad (5)$$

where the diagonal matrix \mathbf{L} defines an approximate kinetic energy smoothing norm [5]. The regularization parameter λ is computed by means of the L-curve criterion [4] as well as generalized cross-validation [1], and the results computed by Tikhonov regularization with the two parameter-choice methods are compared with results computed by means of near-field acoustic holography [2].

In one of our experimental setups, we measured the acoustic pressure from a car tyre rolling at 80 km/h. A total of 977 measurements were recorded on a plane at the side of the tyre as well as on two curved surfaces in the front and the back of the tyre. The BEM discretization of the tyre itself consists of 266 nodes. The BEM discretization as well as the reconstructed normal surface velocity at 60 Hz is shown above, and we note that only the highest 20 dB are displayed. The computed results agree with those from the near-field acoustic holography analysis. More results will be shown in the talk.

References

- [1] G. H. Golub, M. T. Heath and G. Wahba, *Generalized cross-validation as a method for choosing a good ridge parameter*, Technometrics, 21 (1979), pp. 215–223.
- [2] J. Hald, *STSF – a unique technique for scan-based near-field acoustic holography without restrictions on coherence*, Brüel & Kjær Technical Review no. 1 & 2, 1989.

- [3] P. C. Hansen, *Rank-Deficient and Discrete Ill-Posed Problems, Numerical Aspects of Linear Inversion*, SIAM, Philadelphia, 1998.
- [4] P. C. Hansen and D. P. O’Leary, *The use of the L-curve in the regularization of discrete ill-posed Problems*, SIAM J. Sci. Comput., 14 (1993), pp. 1487–1503.
- [5] A. P. Schuhmacher, *Sound Source Reconstructions Using Inverse Sound Field Calculations*, PhD Theses, Report No. 77, July 2000, Ørsted•DTU, Technical University of Denmark.

Estimating fibre process anisotropy

Marcela Hlawiczková (mhlawiczkova@yahoo.com)

Department of Probability and Statistics, Charles University, Praha, The Czech Republik

Viktor Benes (benesv@karlin.mff.cuni.cz)

Department of Probability and Statistics, Charles University, Praha, The Czech Republik

Key words: rose of directions, zonotope, zonoid, fiber process, Prokhorov distance

The anisotropy of 3D fiber processes may be studied by counting intersections of the fiber process with a planar test probe. The 3D problem is reduced to the 2D problem this way.

Let X be a fiber process in 3D space with the length density L_V and the directional distribution R (also called the rose of directions), which is a probability measure. To estimate the rose of directions, the geometrical approach can be used based on zonotopes and zonoids (limits of zonotopes with respect to the Hausdorff metric). Given a rose of directions R , there is a unique zonoid Z corresponding to it. Its support function u is determined by the cosine transformation formula (Goodey & Weil, 1993). Further, there exists a zonotope Z_n with the property that the values of its support function $u_n(n_i)$ in the directions n_i equal the values of the support function $u(n_i)$ of the zonoid Z . Let z_i be the number of intersections of the test plane of a given orientation (normal vectors n_i) with the process X on the unit area of the test plane. The zonotope Z_n may be estimated from the values z_i using the EM-algorithm (Kiderlen, 1999). The probability measure R_n corresponding to the zonotope Z_n is the estimate of the rose of directions. The distance between the true rose of directions and its estimation is measured using the Prokhorov distance (Beneš & Gokhale, 2000).

In the present study, the case of isotropy is considered. The corresponding zonoid Z is then a sphere. The number of intersections between the fiber process and the test probe is evaluated for two test probes (cube, regular octahedron) and realizations of three isotropic fiber processes, for which the edges of 3D Voronoi tessellations generated by various isotropic point processes were chosen. The generating point processes are special cases of Bernoulli cluster fields (BCF, Saxl & Ponížil, 2001) generalizing the Neyman-Scott process of independent clustering (Stoyan et al., 1995) in such a way that the parent points are replaced by point clusters (Matérn globular clusters of the mean cardinality $N = 200$ in the present case) with a probability $0 \leq p \leq 1$. Denoting λ_p the intensity of the parent process, the resulting intensity is $\lambda_B = (1 + p(N - 1))\lambda_p$. BCF's of $p = 0, 1, 0.5$ produce Poisson-Voronoi tessellation (PVT), inhomogeneous tessellation NS200 generated by a standard Neyman-Scott process and the extremely inhomogeneous tessellation B200, respectively. The striking differences between these tessellations are at best revealed by the coefficient of cell volume variation CV_v ; they are 0.42, 3.1 and 7.9 and for PVT, NS200 and B200, respectively.

The tessellations have been constructed in a unit cube by means of the incremental method with the nearest neighbour algorithm (Okabe et al., 1992). The probes were placed in the centre of the cube and their size was chosen such that the edge effects were nearly completely suppressed (the higher is the local inhomogeneity of the tessellation the smaller must be the probe size). The choice of intensities $\lambda_B = 1984, 11\,577$ and $17\,095$ for PVT, NS200 and B200 ensured ≈ 397 intersections for all processes and probes and the number of process realizations was 1000 in all cases.

Using this data, the Prokhorov distance and its pdf were estimated. Two different approaches were chosen:

1. the discrete measure R corresponding to the zonotope in the case when the expected number

of intersections with all test planes is independent of their directions (cube for a cubic probe, tetrakaidecahedron for an octahedral probe),

- the continuous measure R represented by the zonoid (i.e. by sphere in the considered case).

The results obtained for discrete measure approach are shown in Fig. 1. The effect is clearly manifested of the local inhomogeneity of the examined processes on the distributions of the Prokhorov distances - see Tab. I. The mean value and the standard deviation of PVT edges are significantly smaller than these ones of NS200 and B200 edges. In the latter two inhomogeneous cases, the difference in the two discrete measures is clearly revealed. In a high number of realizations, the Prokhorov distance corresponds to the angles between the normal vectors of zonotope Z faces ($\pi/2$ for cube and 0.95, 1.23 for octahedron) and is represented by peaks in the histogram. The continuous measure approach is presented in Fig. 2. The local inhomogeneity has the same effect as in the discrete case. It can be seen that the values of Prokhorov distance are shifted from zero to higher values, because discrete and continuous measures are compared here. The estimation of Prokhorov distance and its minimum value are based on the evaluation of the sphere covering by spherical caps. The Prokhorov distance of a significant number of fiber processes realizations equals this minimum value. The mean values and standard deviations for all investigated cases are shown in the Tab. I.

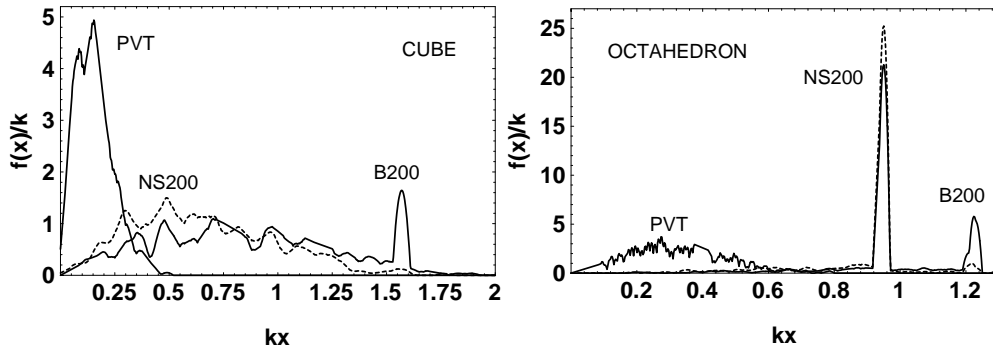


Figure 1: Probability density functions $f(x)$ of the Prokhorov distances in the discrete approach; $k = 2\pi$.

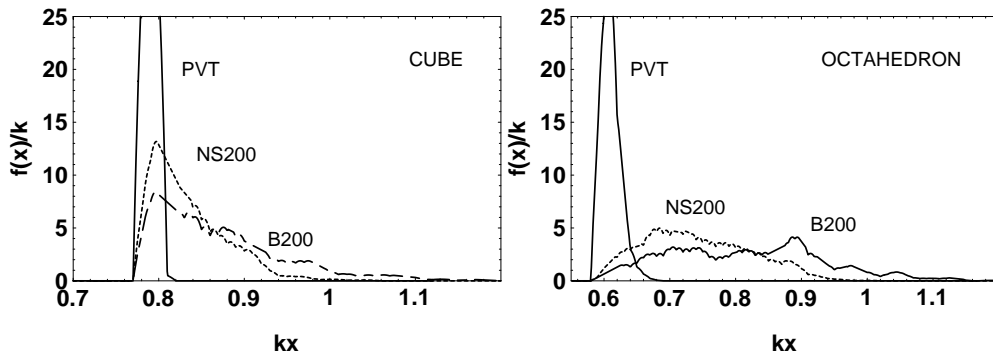


Figure 2: Probability density functions $f(x)$ of the Prokhorov distances in the continuous approach; $k = 2\pi$.

Tab. I Prokhorov distances P and their standard deviations
in the *discrete* and *continuous* cases

tess.	EP_{dis}		SDP_{dis}		EP_{con}		SDP_{con}	
	<i>oct. cub.</i>		<i>oct. cub.</i>		<i>oct. cub.</i>		<i>oct. cub.</i>	
PVT	0.053	0.025	0.024	0.014	0.097	0.126	0.005	0.002
NS200	0.142	0.105	0.029	0.053	0.118	0.133	0.015	0.006
B200	0.154	0.137	0.033	0.068	0.131	0.138	0.019	0.011

References

- Beneš, V. & Gokhale, A. (2000) *Kybernetika* 36, p. 149.
- Goodey, P. & Weil, W. (1993) In P.M. Gruber, J.M. Wills (eds.): *Handbook of Convex Geometry*, p. 1297.
- Kiderlen, M. (1999) Dissertation. Universität Karlsruhe.
- Okabe, A., Boots, B. & Sugihara, K. (1992) *Spatial tessellations*. J.Wiley & Sons, Chichester.
- Saxl, I. & Ponížil, P. (2001) *Materials Characterization* (in press).
- Stoyan, D., Kendall, W.S. & Mecke, J. (1995) *Stochastic Geometry and its Applications*. J. Wiley & Sons, New York.

Discrete inversion of the spherical cosine transform in stereology

Markus Kiderlen (kiderlen@imf.au.dk)

Mathematical Institute, University of Karlsruhe, Germany

Several Stereological questions lead to the problem to estimate a (positive) measure on the unit sphere from (approximate) values of its cosine transform in finitely many directions. In the talk, a short introduction to the geometric background of the problem will be given. Then, a nonparametric maximum likelihood method will be presented. The resulting estimator is a discrete measure on the unit sphere, which can be calculated numerically using the EM algorithm. Under some mild conditions on the input data we will show consistency for this estimator. Simulations will illustrate the methods.

Bayesian inversion of piecewise affine inverse problems

Odd Kolbjørnsen (ok@math.ntnu.no)

Department of Mathematical Sciences, Norwegian University of Science and Technology, Trondheim, Norway

Henning Omre (omre@math.ntnu.no)

Department of Mathematical Sciences, Norwegian University of Science and Technology, Trondheim, Norway

Abstract

Piecewise affine inverse problems are solved in Bayesian framework with Gaussian random field priors and a Gaussian likelihood. The posterior distribution for this problem is not Gaussian because of the nonlinearity in the problem. An algorithm to sample the posterior for piecewise affine inverse problems is defined under Gaussian assumption.

Introduction

Inverse problems arise in many scientific problems and engineering applications. An inverse problem is obtained when the observations are related to transforms of the object of interest. Let the object of interest be a function, z , assumed to be in a function space Z . The observations are then $o = \omega(z) + \varepsilon$, with $\omega: Z \rightarrow \mathbf{R}^r$ being the known forward map of the inverse problem, and $\varepsilon \in \mathbf{R}^r$ being observation error.

The Bayesian approach to inverse problems, is in principle no different from the Bayesian approach to any other problem, see Gelman et al. (1995). The analyzer must specify a prior, $D\{Z\}$, on the parameter space Z and a likelihood, $D\{O|Z = z\}$, for the observations. The posterior distribution, $D\{Z|O = o\}$, is the Bayesian answer to an inverse problem. A common way of representing the posterior is through a finite sample. For general nonlinear inverse problems, the posterior is usually sampled by the use of a general purpose algorithm such as rejection sampling, resampling schemes or Markov chain based methods. When the observations are measured with high precision, many general purpose algorithms experience problems and fail for the case of exact observations. When explicit choices have been made for the prior and the likelihood, specialized algorithms may be implemented to overcome these problems.

The problem

In the current presentation the inverse problem is assumed to be piecewise affine. Piecewise affine inverse problems are very general. In particular inverse problems having a variational structure, such as the Fermat principle of travel time tomography can be phrased as piecewise affine inverse problems. In the current setting a solution is sought for the case of a Gaussian random field prior on Z and a Gaussian likelihood. A similar problem was investigated by Kolessa (1986) in a slightly different setting.

An inverse problem is classified as piecewise affine if the forward map of the problem is a piecewise affine operator.

Definition 1 (Piecewise affine operator) An operator $\omega : Z \rightarrow \mathbf{R}^r$, is said to be piecewise affine, if it can be represented in the following way:

$$\omega(z) = B_x z + b_x \text{ for } z \in A_x; \quad x \in X$$

with X being an index set, $\{A_x\}_{x \in X}$ being a partition of Z ; $B_x : Z \rightarrow \mathbf{R}^r$ being bounded linear operators on Z and b_x being r dimensional vectors. The indexed set of triplets $\{A_x, B_x, b_x\}_{x \in X}$ are the parameters of the piecewise affine operator.

The type of piecewise affine inverse problems depend on the index set X . For the case $X = \{1\}$ it correspond to linear inverse problems, for $X \neq \{1\}$ they constitute a general class of nonlinear inverse problems. In current work both $X = \{1, 2, \dots, m\}$ and $X \subset \mathbf{R}^d$ is considered.

The results

The posterior distribution is calculated to be a mixture of truncated Gaussian distributions both in the case of a finite index and in the case of a continuous index.

For the finite index case, $X = \{1, 2, \dots, m\}$, a mixing distribution on X can be explicitly calculated, and an algorithm based on rejection sampling that produces exact independent samples from the posterior can be provided.

In the case of a continuous index, $X \subset \mathbf{R}^d$, more attention must be given to the partition $\{A_x\}_{x \in X}$. Under the right assumptions there also exist a mixing distribution for this case, however the distribution must be extended beyond X to deal with the continuous dependence on x in the partition (Adler 1981). Moreover as a part of the final sampling algorithm a distribution that is only known to proportionality must be sampled by the use of general purpose algorithms. This distribution is however of finite dimension, and nonsingular even for the case of exact observations, which is a substantial improvement on the initial problem.

Example

A meteorologist want to reconstruct the temperature field of the previous day. The observations at hand, are the temperatures each morning and the global extremes in between.

A stochastic model for the temperature during one day, $t \in [0, 24]$ is described by,

$$Z(t) = Z_0 + Z_1 \sin \frac{\pi t}{12} + Z_2 \cos \frac{\pi t}{12} + \tilde{Z}(t),$$

with Z_0, Z_1, Z_2 and $\tilde{Z}(t)$ being independent; $Z_0 \sim N(15, 5^2)$, $Z_1 \sim N(5, 2^2)$, $Z_2 \sim N(0, 0.5^2)$, and $\tilde{Z}(t)$ is a zero mean residual stochastic field with covariance function $C_{\tilde{Z}}(t, t+h) = \exp\{-3|h/4|^2\}$. Figure 1 shows 200 samples from this prior distribution. Assume $z(0) = 19.78$, $z(24) = 19.74$, $\max_{0 \leq t \leq 24} z(t) = 26.04$ and $\min_{0 \leq t \leq 24} z(t) = 16.61$ is observed, and that the observations are exact.

The posterior was sampled in three steps. Firstly the location of the extremal points and the second derivative at these points was sampled according to a distribution known up to a constant, this was done using a SIR algorithm. Secondly the Gaussian random field was sampled conditioned to linear constraints imposed by the problem. In the last step the sample was accepted if the minimum and the maximum values of the obtained sample where the values observed. In the third step 43.8% of the samples where accepted. In Figure 2, 400 samples from the posterior are shown. For this particular problem general purpose algorithms does not work.

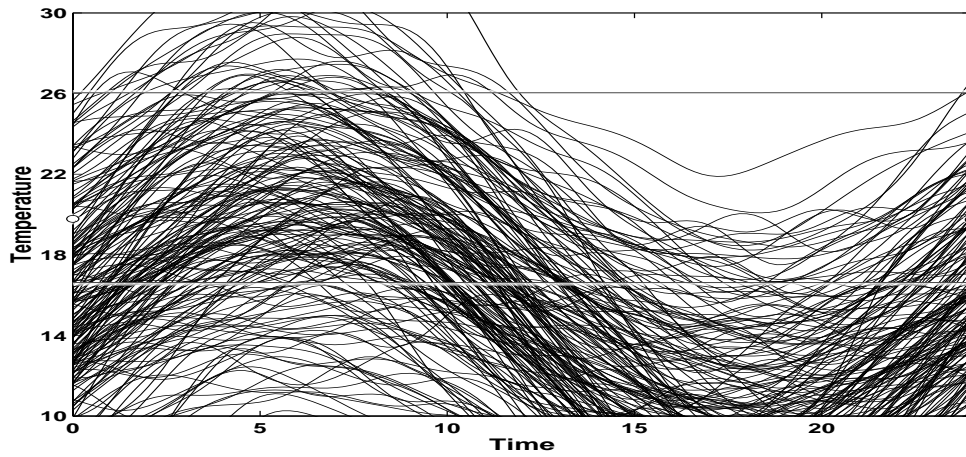


Figure 1: The Figure shows 200 samples from the prior distribution of the example. The horizontal lines shows the observed level of maximum and minimum values. The white circles at each end, show the values observed at the boundaries. Some of samples from the prior are partially or completely outside the scaling of the figure.

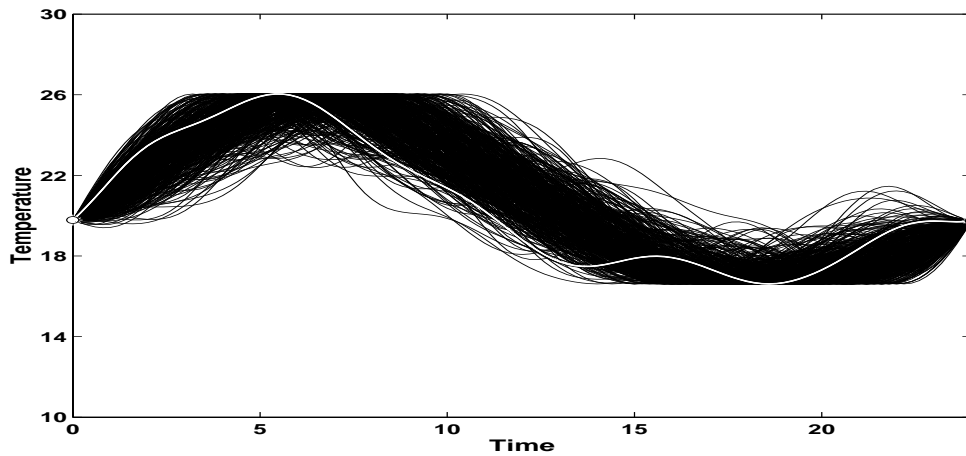


Figure 2: The figure show 400 realizations from the posterior distribution from the example. The white curve is the actual path.

References

Adler, R.J. (1981), "The geometry of random fields"; Wiley.

Gelman, A., Carlin, J., Stern, H., and Rubin, D.B. (1995), "Bayesian data analysis"; London; Chapman & Hall.

Kolessa A.E. (1986), "Recursive filtering algorithms for systems with piecewise linear non-linearities", *Avtomat. Telemekh.*, 4, 48-55.

3D surface reconstruction as Bayesian inversion

Robin D. Morris (rdm@ptolemy.arc.nasa.gov)

NASA Ames Research Center, California, USA

Vadim Smelyanskiy, Peter Cheeseman and David Maluf

NASA Ames Research Center, California, USA

The problem of three dimensional surface reconstruction from images can be formulated as an inversion problem – inverting the image formation process. From a Bayesian viewpoint, the problem becomes one of estimating the parameters of a surface model from observations (images) of that model. In this talk I will show how a computer model of the forward problem (going from a model to an image, the computer graphics problem of rendering) can be augmented to also compute the derivatives of the image pixel values with respect to the 3d surface model parameters. This allows us to efficiently invert the process and infer the MAP surface estimate. It also allows us to reconstruct the 3d model at any scale that is justified by the data, including the super-resolved case, where many surface elements project into a single pixel in each of the (many) low-resolution images.

Consider a height field surface described by a regular triangular mesh. At each vertex of the mesh we store the values of the height and the albedo, so the surface is $\{\mathbf{z}, \rho\}$. We group the heights and albedos into a vector \mathbf{u} . Applying Bayes Theorem gives

$$p(\mathbf{u}|I_1 \dots I_n) \propto p(I_1 \dots I_n|\mathbf{u})p(\mathbf{u}), \quad (6)$$

where I_i are the observed images.

We assume that the likelihood results from Gaussian residuals, and use a simple smoothing prior on \mathbf{u} that penalizes curvature. The negative log-posterior is then

$$L(\mathbf{u}) = \frac{1}{2\sigma_f^2} \sum_{f,p} (I_{f,p} - \hat{I}_{f,p}(\mathbf{u}))^2 + \mathbf{x}Q\mathbf{x}^T \quad (7)$$

where p indexes the pixels. The formation of $\hat{I}(\mathbf{u})$ is the computer graphics process of rendering, and so clearly $L(\mathbf{u})$ is a nonlinear function of \mathbf{u} . To make progress with finding the MAP estimate, we linearize the rendering process about the current estimate \mathbf{u}_0 , to give

$$\hat{I}(\mathbf{u}) = \hat{I}(\mathbf{u}_0) + \mathbf{D}\mathbf{x} \quad (8)$$

where \mathbf{D} is the matrix of derivatives, $\partial \hat{I}_{f,p} / \partial \mathbf{u}_i$; and $\mathbf{x} = \mathbf{u} - \mathbf{u}_0$. This linearization turns the problem into the minimization of a quadratic form, which can be performed using, for example, conjugate gradient. At the convergence of the minimization the new estimate for \mathbf{u} can be used as \mathbf{u}_0 and the process iterated. We have found that four or five iterations are usually sufficient.

It now remains to describe how to compute the image, $\hat{I}(\mathbf{u})$, and the derivative matrix \mathbf{D} . Computing an image from a triangulated mesh description of a surface is a well studied problem in computer graphics [1]. However, because of the emphasis in computer graphics of producing a visually appealing image quickly, much modern computer graphics is unsuitable, and we must return to the early work, when computation was done in *object space*. The brightness of a pixel in the image is a sum of the contributions from individual surface triangles whos projection overlaps the pixel

$$\hat{I}_p = \sum_{\Delta} f_{\Delta}^p \Phi_{\Delta} \quad (9)$$

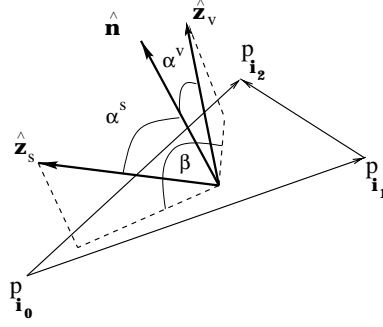


Figure 1: Geometry of the triangular facet, illumination direction and viewing direction. $\hat{\mathbf{z}}_s$ is the vector to the illumination source; $\hat{\mathbf{z}}_v$ is the viewing direction.

where Φ_Δ is the radiation flux reflected from the triangular facet Δ and received by the camera, and f_Δ^p is the fraction of that flux that falls into pixel p .

$$\begin{aligned}\Phi_\Delta &= \rho E(\alpha^s) \cos \alpha^v \cos^\kappa \theta \Delta \Omega, \\ E(\alpha^s) &= A(I^s \cos \alpha^s + I^a), \\ \Delta \Omega &= S/d^2.\end{aligned}\tag{10}$$

where α^s, α^v are respectively the angles between the normal to the triangle and the illumination direction, and the normal to the triangle and the viewing direction, θ is the angle between the camera axis and the viewing direction, and κ is the lens falloff factor, see figure 1. We assume Lambertian reflection, and ρ is the albedo of the triangle. A is the area of the triangle, I^s, I^a are the intensities of the direct and ambient light, and $\Delta \Omega$ is the solid angle subtended by the lens.

To compute the image intensities we therefore need to compute the areas of the polygons which are the intersections of the pixel boundaries and the projection of the triangles onto the pixel plane. This is an exercise in computational geometry [2]. To compute the derivative matrix we need to take derivatives of equation 9. The derivatives with respect to the albedo components of \mathbf{u} are straightforward. The derivatives with respect to the height components are more complex. They have two distinct contributions

$$\frac{\partial \hat{I}_p}{\partial z_i} = \sum_{\Delta} \left(f_\Delta^p \frac{\partial \Phi_\Delta}{\partial z_i} + \Phi_\Delta \frac{\partial f_\Delta^p}{\partial z_i} \right).\tag{11}$$

Variation of the height of a vertex of a triangle gives rise to variations in the normal of the triangle, and this produces the derivatives of the total radiation flux Φ_Δ . Variation in the heights also gives rise to displacements of the projection of that point in the image plane, and hence changes in the areas of the polygons with edges containing this point. This produces the derivatives of the area fractions f_Δ^p .

The flux derivative can be computed directly from the coordinates of the triangle vertices and the camera position. Computation of the derivatives of the projected area fraction necessitates considering how the projection of the vertex on the image plane moves as the vertex height changes, ie the point displacement derivative, $\partial \mathbf{P} / \partial z_i$. Then

$$\frac{\partial f_\Delta^p}{\partial z_i} = \frac{1}{A_\Delta} \left(\frac{\partial A_{\text{polygon}}}{\partial \mathbf{P}_i} - f_\Delta^p \frac{\partial A_\Delta}{\partial \mathbf{P}_i} \right) \frac{\partial \mathbf{P}_i}{\partial z_i}\tag{12}$$

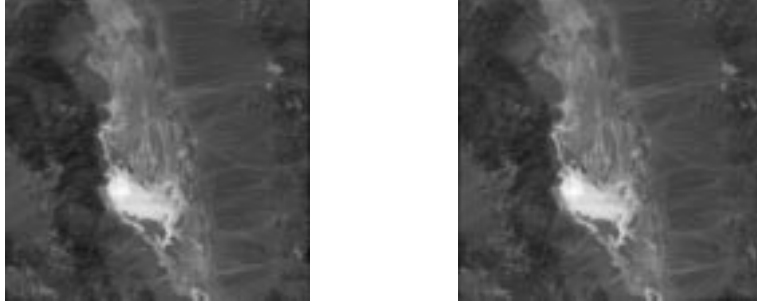


Figure 2: Two images rendered from the synthetic Death Valley surface

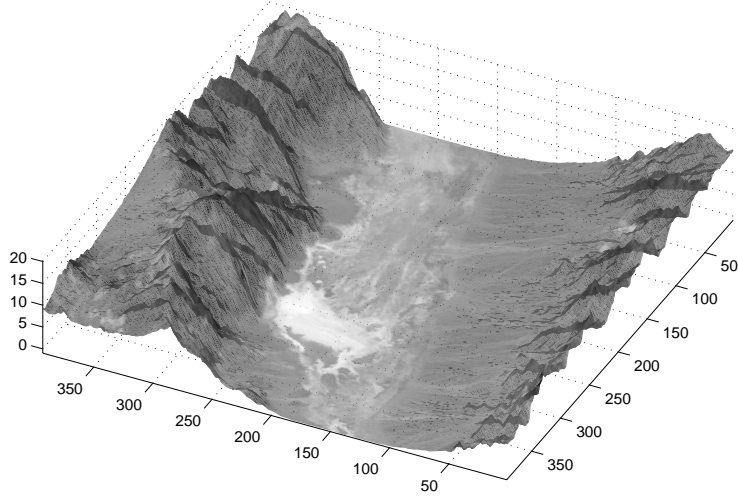


Figure 3: Surface reconstructed from the images in figure 2

which shows that to compute the derivative of the area fraction we need to compute the derivative of the triangle area, A_{Δ} , and the polygon areas, A_{polygon} . These derivatives can be computed by a very general algorithm that considers one edge of the polygon at a time, and accumulates the contributions to the derivative.

The point displacement derivatives, $\partial \mathbf{P} / \partial z_i$ can be derived from the definition of the simple perspective sensor [3], where

$$\mathbf{P}_x = \frac{[\mathbf{A}\mathbf{R}(\mathbf{P} - \mathbf{t})]_x}{[\mathbf{R}(\mathbf{P} - \mathbf{t})]_z} \quad (13)$$

\mathbf{A} is the matrix of camera internal parameters, \mathbf{R} is the rotation matrix and \mathbf{t} the position of the camera. The point displacement derivatives are given in [4].

Figure 2 shows two of the four images rendered from an artificial surface. The surface was generated by taking a USGS digital elevation model for Death Valley, and using the intensities from a co-registered Landsat-TM image as surrogates for the albedos. Figure 3 shows the surface reconstructed from the four images. Further details can be found in [5].

References

- [1] J. Foley, A. van Dam, S. Finer, and J. Hughes. *Computer Graphics, principles and practice*. Addison-Wesley, 2nd ed. edition, 1990.
- [2] J. O'Rourke. *Computational Geometry in C*. Cambridge University Press, 1993.
- [3] G. Xu and Z. Zhang. *Epipolar Geometry in Stereo, Motion and Object Recognition*. Kluwer, 1996.
- [4] R.D. Morris, V.N. Smelyanskiy and P.C. Cheeseman. *Matching Images to Models – Camera Calibration for 3-D Surface Reconstruction*. Submitted to EMMCVPR 2001, Sophia Antipolis, September 2001.
- [5] V.N. Smelyanskiy, P. Cheeseman, D.A. Maluf and R.D. Morris. *Bayesian Super-Resolved Surface Reconstruction from Images*. In Proceedings of Conference on Computer Vision and Pattern Recognition, Hilton Head Island, 2000 (CVPR 2000).

Geophysical applications of MCMC: Bayesian calculations and MC-optimization with slow forward algorithms

Klaus Mosegaard (klaus@gfy.ku.dk)

Department of Geophysics, University of Copenhagen, Denmark

Monte Carlo methods are becoming increasingly important for solution of non-linear inverse problems in two different, but related, situations. In the first situation we need a near optimal solution (measured in terms of data fit and adherence to given constraints) to the problem. In the second situation, the inverse problem is formulated as a search for solutions fitting the data within a certain tolerance, given by data uncertainties. In a non-probabilistic setting this means that we search for solutions with calculated data whose distance from the observed is less than a fixed, positive number. In a Bayesian context, the tolerance is “soft”: a large number of samples of statistically near-independent models from the a posteriori probability distribution are sought. Such solutions are consistent with the data as well as the available prior information.

Early examples of solution of inverse problems by means of Monte Carlo methods are abundant in geophysics and other disciplines of applied physics. Since *Keilis-Borok and Yanovskaya* [1967] and *Press* [1968, 1971] made the first attempts at randomly exploring the space of possible Earth models consistent with seismological data, there has been considerable advances in computer technology, and therefore an increasing interest in these methods. Recently, Bayes theorem and the Metropolis algorithm have been used for calculating approximate a posteriori probabilities for inverse problems (see, e.g., *Pedersen and Knudsen* [1990], *Koren et al.* [1991], *Gouveia and Scales* [1998], *Dahl-Jensen et al.* [1999], *Khan et al.* [2000], *Rygaard-Hjalsted et al.* [2000], and *Khan and Mosegaard* [2001]).

Most applications of Monte Carlo Methods for inversion suffer from the major problem that misfit calculations are so computer intensive, and the model parameter space is so vast, that, in practice, only relatively few models can be sampled. This has led to the development of methods that seek to obtain (in some sense) optimum results within a given (fixed) number of iterations. Some of the most successful of these methods are based on ideas borrowed from statistical mechanics (*Nulton and Salamon* [1988]).

Bayesian inversion of boundary value data

Geoff Nicholls (nicholls@math.auckland.ac.nz)

Department of Mathematics, University of Auckland, New Zealand

Colin Fox (fox@math.auckland.ac.nz)

Department of Mathematics, University of Auckland, New Zealand

Electrical conductivity imaging is one of several non-invasive imaging techniques in which an object is probed by irradiating it with waves of current, heat or ultrasound, and measurements are made of the scattered field. The imaged quantity σ is then related to the wave field u by

$$\begin{aligned} \text{Electrical} \quad \nabla \cdot \sigma \nabla u &= 0 \\ \text{Thermal} \quad \nabla \cdot \sigma \nabla u &= \frac{\partial u}{\partial t} \\ \text{Acoustic} \quad \nabla \cdot \sigma \nabla u &= \frac{\sigma}{c^2} \frac{\partial^2 u}{\partial t^2} \end{aligned}$$

In each of these canonical expressions the “forward problem” (from σ to u) requires solution of the corresponding boundary, or initial-boundary value problem in two or three dimensions. To recover the image, σ we must solve the “inverse problem”, which is ill-posed and non-linear.

Exact inverses have been found for some of these problems (see for example [3]). However, analysis shows that the linearised forward problems above have singular values that decrease at least geometrically (for example [1]) and hence any inverse must be discontinuous and will give images dominated by noise. This inherent ill posed behaviour is actually severe since, in the presence of noise, only a limited amount of information about σ is transmitted through the forward map. Consequently, any image reconstruction algorithm must provide information that is not available in the measurements. To make best use of the information that is measurable, algorithms must use accurate models of both the forward map and noise process. Finally, we would like to quantify uncertainty in our “solution”. A solution is not a single image, it is a distribution over more or less plausible images. We are not aware of any inferential framework which meets all these criteria, unless it be an essentially Bayesian inferential scheme, with a physics-based likelihood.

New sampling methodologies open up the possibility of sampling distributions involving such likelihoods, and thereby carrying out sample-based Bayesian inference. We focus on the conductivity imaging problem, and a corresponding family of Markov chain Monte carlo algorithms. Such algorithms require millions of likelihood ratio evaluations, in each of which a number of Green’s functions must be computed. Over the last few years, we have been investigating methods to make this iterative calculation tractable. We are particularly concerned with the order of one likelihood ratio calculation, as a function of the number of elements in the finite element and boundary element schemes used to solve for the Green’s function of the forward problem. It seems hard to go past a local linearisation scheme [2], which is order constant in the number of elements. However, we will discuss a wide range of Markov chain Monte carlo schemes, including Langevin and hybrid algorithms, and algorithms related to continuous time MCMC, and consider how they may be coupled to numerical methods for solving the forward boundary value problem.

In order to solve an inverse problem, it is not necessary to invert anything, except possibly our way of thinking.

References

- [1] C. Fox. *Conductance Imaging*. PhD thesis, University of Cambridge, 1989.
- [2] C. Fox and G. K. Nicholls. Sampling conductivity images via MCMC. In K.V. Mardia, R.G. Ackroyd, and C.A. Gill, editors, *The Art and Science of Bayesian Image Analysis*, Leeds Annual Statistics Research Workshop, pages 91–100. University of Leeds, 1997.
- [3] J. Sylvester and G. Uhlman. A global uniqueness theorem for an inverse boundary value problem. *Ann. Math.*, 125:643–667, 1987.

Posterior distributions for numerical weather forecasts

Douglas Nychka (nychka@cgd.ucar.edu)

National Center for Atmospheric Research, Boulder, USA

Thomas Bengtsson and Chris Snyder

National Center for Atmospheric Research, Boulder, USA

Given sparse irregular observation functionals of the atmosphere, the goal is to update the estimate of the current state of the atmosphere and then to use this update to forecast ahead in time. The updating step is a huge inverse problem, perhaps the largest solved on a routine basis; the number of observations is on the order of 10^5 and the state vector describing the atmosphere is 10^6 . This talk reports our research to find computable, Bayesian solutions to this problem. The focus is on an ensemble technique (i.e. Monte Carlo sampling) to estimate reasonable regularizing penalties that adapt to the changing state of the atmosphere and provide credible posterior probabilities. An interesting statistical problem is to estimate regularization parameters sequentially because the large size of this problem does not allow for storage of previous forecasts.

Ensemble forecasting is used in numerical weather prediction to give an improved estimate of the atmospheric state and provide measures of forecast accuracy. Essentially one carries along a set of forecasts where the spread among the group is a measure of forecast uncertainty and the group mean is interpreted as the best single forecast. While the method is effective, there are some fundamental issues in interpreting the ensemble as a statistically valid representation of uncertainty in the state of the atmosphere. In Bayes language, in what sense does the distribution among ensemble members approximate a posterior distribution for the state vector? Coupled with this interpretation is the difficulty in the specification of large, complex covariance matrices used to combine a numerical forecast with observed data. We approach this problem by representing the prior distribution as a mixture of Gaussian distributions, then generate an ensemble as a random sample from the posterior. A crucial step in this process to go backwards from an ensemble to a prior distribution for the next forecast cycle. Here we use a kernel density estimate. The bandwidth in this kernel approximation is an important tunable parameter and we construct a sequential estimate using discrepancies between the forecasts and the observed data.

Bayesian inversion in reservoir characterization with complex forward models

Henning Omre (omre@math.ntnu.no)

Department of Mathematical Sciences, Norwegian University of Science and Technology, Trondheim, Norway

Ole Petter Lødøen (olelod@math.ntnu.no)

Department of Mathematical Sciences, Norwegian University of Science and Technology, Trondheim, Norway

Problem setting

Reliable forecasts of production from petroleum reservoirs are crucial for efficient reservoir management. These forecasts must be based on general reservoir knowledge and reservoir specific observations.

Consider a reservoir with production start at time t_0 , and let time for evaluation be t_e , with $t_e \geq t_0$. The production variables, containing oil production-rate, gas-oil ratio, bottom-hole pressure etc., is termed $p_t; t \in [t_0, \infty)$. The production is crucially dependent on the reservoir variables, $r_x, x \in D$, containing porosity, permeability etc. in the three dimensional reservoir domain D . The reservoir specific observations contain seismic amplitude data covering D , d_s ; observations along the well trace, d_w ; and production history observed in time $[t_0, t_e)$, d_p .

Focus of the study is on forecasting future production, $p_t; t \in [t_e, \infty)$, termed p_{t+} , based on the available information. The time reference, t , is continuously defined, but in practice p_t will be a finite-dimensional vector on a grid along the time axis.

Stochastic model

The problem is solved in a Bayesian inversion setting, see Omre and Tjelmeland (1997), and the model is presented in the graph in Figure 1.

A prior model for the reservoir variables, R_x , is represented by the probability density function (pdf), $f(r_x)$. These variables are linked to the production variables by a fluid flow simulator, $P_t = \omega(R_x)$. Implicitly in this is a recovery strategy for oil, i.e. a well design and injection procedure, defined. The simulator is assumed to be perfect, i.e. it links P_t and R_x without error, $f(p_t|r_x)$. The reservoir specific observations are linked to (P_t, R_x) through likelihood models $f(d_s|r_x)$, $f(d_w|r_x)$ and $f(d_p|p_t)$. The two former are defined in Eide et al.(1999) and Buland and Omre (2000). The latter represents p_t in the time interval $[t_0, t_e)$, termed p_{t-} , with an additive Gaussian observation error.

The reservoir is usually evaluated at two stages:

- Appraisal stage, with $t_e = t_0$, and the posterior pdf of interest being:

$$f(p_t|d_s, d_w) = \int f(p_t|r_x)f(r_x|d_s, d_w)dr_x \quad (14)$$

- Production stage, with $t_e \geq t_0$, and the posterior pdf of interest being:

$$f(p_{t^+}|d_s, d_w, d_p) = f^{-1}(d_p) \int \int f(d_p|p_{t^-})f(p_{t^-}|r_x)f(p_{t^+}|r_x)f(r_x|d_s, d_w)dr_x dp_{t^-} \quad (15)$$

Sampling procedure

The posterior models are not analytically tractable, primarily due to strong non-linearity in the fluid flow simulator $\omega(\cdot)$. Moreover, it may take days, or even weeks, to run one forward model in $\omega(\cdot)$. This makes general purpose sampling algorithms like rejection sampling, SIR, Kitandis-Oliver algorithm and MCMC-algorithms unsuitable, see Omre (2000).

In order to improve the sampling, an approximate fluid flow simulator is defined, $p_t^* = \omega_*(r_x)$. This may be done by solving the differential equations involved on a coarser mesh. The production variables are assumed to be linked to the approximate ones through,

$$f(p_t|p_t^*) \rightarrow \text{Gauss}(A_* p_t^*, \Sigma_*) \quad (16)$$

with A_* and Σ_* being unknown parameters.

The forecast of production can then be written as:

- appraisal stage:

$$f(p_t) = \int f(p_t|p_t^*)f(p_t^*)dp_t^* \quad (17)$$

- production stage:

$$f(p_{t^+}|d_p) = f^{-1}(d_p) \int \int f(d_p|p_{t^-})f(p_{t^-}|p_t^*)f(p_{t^+}|p_t^*)f(p_t^*)dp_{t^-} dp_t^* \quad (18)$$

The conditioning on (d_s, d_w) is implicitly done through p_t^* and is not shown in the notation.

The following sampling is performed:

$$r_x^i; i \in \{1, \dots, n\} \text{ iid } f(r_x|d_s, d_w) \quad (19)$$

and

$$p_t^{*i} = \omega_*(r_x^i); i \in \{1, \dots, n\} \quad (20)$$

This can be done with small computational cost even for large n . Based on this, an estimate of the pdf $f(p_t^*)$ can be made: $\hat{f}(p_t^*)$.

Consider $\{1, \dots, m\}$ being a subset of $\{1, \dots, n\}$ with $m \ll n$. Compute:

$$p_t^j = \omega(r_x^j); j \in \{1, \dots, m\} \quad (21)$$

Each computation will be very computationally expensive. Based on $(p_t^j, p_t^{*j}); j \in \{1, \dots, m\}$ estimates for A_* and Σ_* can be made and hence an estimate $\hat{f}(p_t|p_t^*)$ can be obtained. Note that the selection of the subset $\{1, \dots, m\}$ among $\{1, \dots, n\}$ may be optimized.

The estimated forecasts of production can be based on:

- appraisal stage:

$$\hat{f}(p_t) = \int \hat{f}(p_t | p_t^*) \hat{f}(p_t^*) dp_t^* \quad (22)$$

- production stage:

$$\hat{f}(p_{t+} | d_p) = f^{-1}(d_p) \int \int f(d_p | p_{t-}) \hat{f}(p_{t-} | p_t^*) \hat{f}(p_{t+} | p_t^*) \hat{f}(p_t^*) dp_{t-} dp_t^* \quad (23)$$

The former estimate is straight forward to compute. While the latter can be determined by a procedure similar to the SIR algorithm. Note that the uncertainty related to using the approximate fluid flow simulator instead of the correct one will be reflected in the production forecast uncertainty.

Example

The example is based on the study in Hegstad and Omre (1999). The setting is as in Figure 1. The correct fluid flow simulator, $\omega(\cdot)$, is based on a $(50 \times 50 \times 15)$ discretization, and each run requires 24 hours processing time. The approximate simulator, $\omega_*(\cdot)$, is based on a $(10 \times 10 \times 15)$ discretization and can be run in less than five minutes.

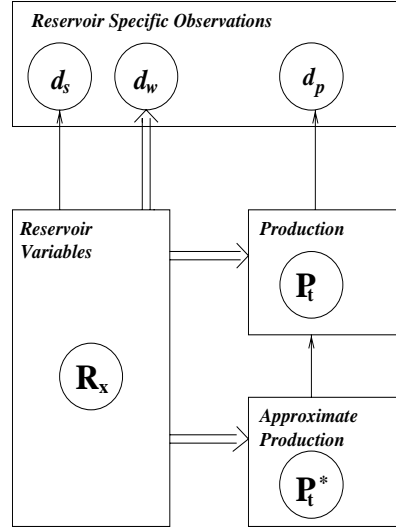


Figure 1: Graph of stochastic reservoir model.

The production from a reference reservoir taken to be the truth is presented in Figure 2. There is one vertical injection well in which the bottom-hole pressure is monitored, and two horizontal production wells in which oil production-rate and gas-oil ratio are monitored. Evaluation time, t_e , is at 1491 days, hence the production plotted with solid lines are observed.

In the study, $n = 100$, i.e. one hundred runs of the approximate simulator $\omega_*(\cdot)$, and $m = 5$, i.e. five runs of the correct simulator, $\omega(\cdot)$, are run. The estimate $\hat{f}(p_t | p_t^*)$ is obtained and evaluated against independent runs of $\omega(\cdot)$. One typical case is shown in Figure 3. Note that the forecast is improved relative to using P_t^* only. The accuracy is improved on the cost of precision.

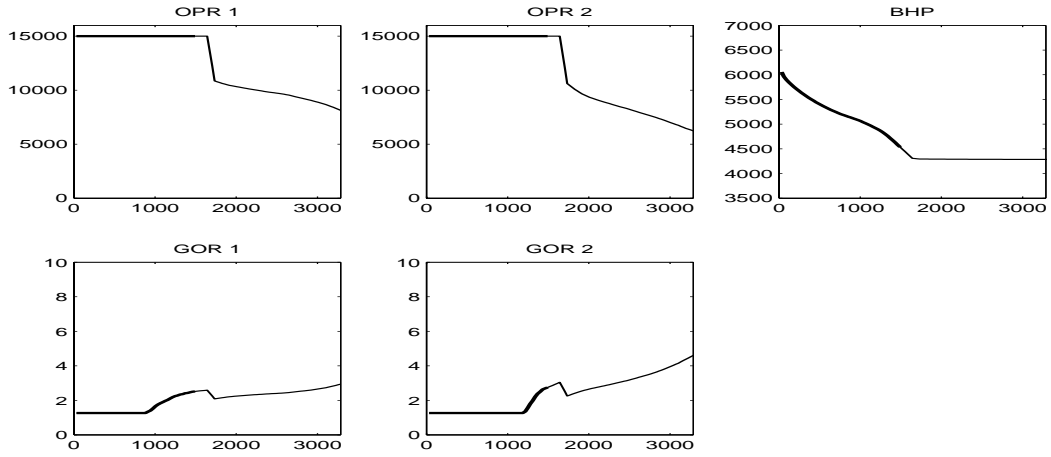


Figure 2: Production variables from reference reservoir

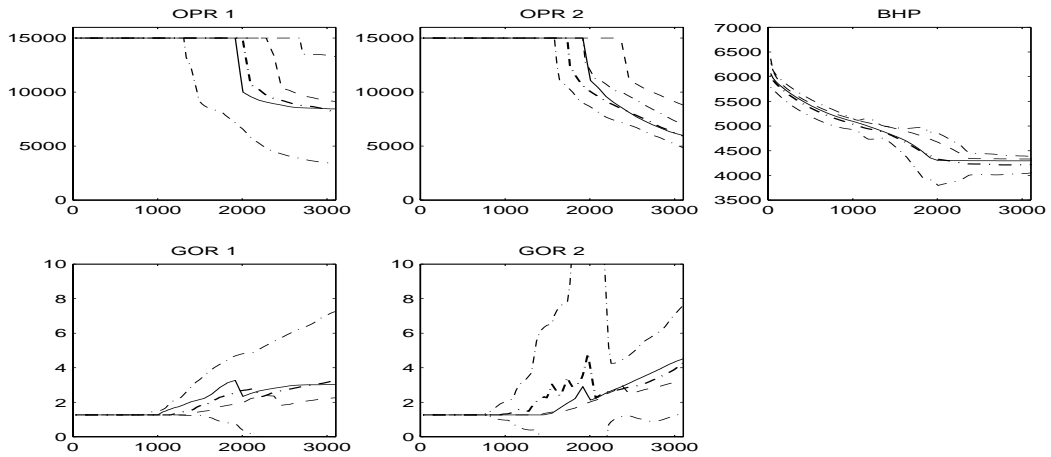


Figure 3: Forecast of one arbitrary realization, r_x .
 $p_t = \omega(r_x)$:—; $p_t^* = \omega_*(r_x)$:---; $\hat{f}(p_t | p_t^*)$: exp - - - - , 0.80 interval - - - -

In Figure 4, estimated forecast of production, $\hat{f}(p_{t+}|d_p)$, is presented. Note that if only $m = 5$ runs of the correct simulator are possible, none of the general purpose sampling algorithms can be used.

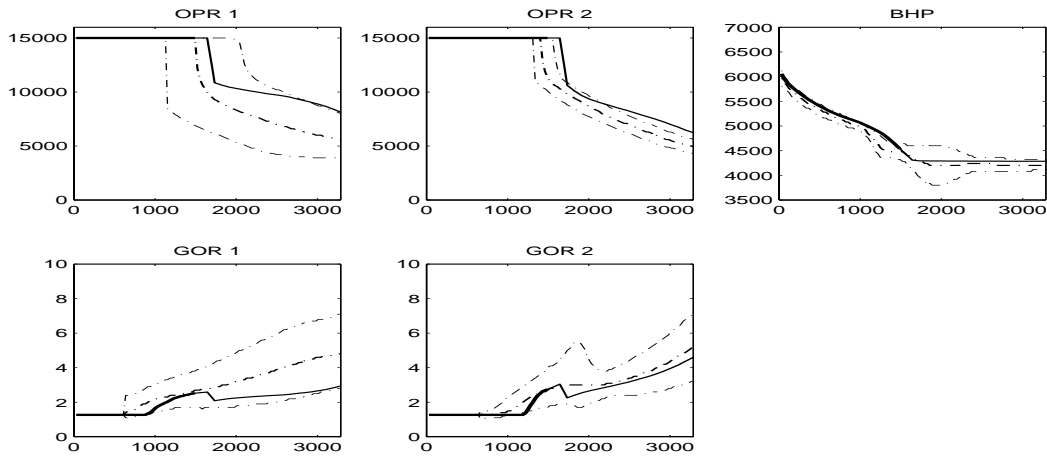


Figure 4: Forecast at production stage: $\hat{f}(p_{t+}|d_p)$: exp $\cdots\cdots$, 0.80 interval $\cdots\cdots$.
Reference production: observed — , future ---

References

See www.math.ntnu.no/~omre/recentwork.html and references therein.

Quantitative analysis of data from PET imaging studies

Finbarr O'Sullivan (finbarr@stat.ucc.ie)

Department of Statistics, University College Cork, Ireland

Positron emission tomography (PET) is a radiological imaging technique that has the ability to measure metabolic characteristics of tissue in-vivo. Statisticians are familiar with the reconstruction problem of PET which involves the inversion of the Radon transform based on scaled Poisson data to produce estimates of the distribution of activity of an injected radio-tracer.

Data sets arising from PET studies involve dynamic volumetric scans representing the temporally integrated time-course of the distribution of a radiotracer and its metabolites in a tissue region. Dose constraints on the injected radio-tracer place critical limitations on the spatial and temporal accuracy of the data. In modern PET machines the nominal spatial resolution of scans is between 2 and 5mm. Temporal sampling varies with the radiotracer used - there can be as many as 1 scan per second to perhaps as few as 2 scans per hour. A typical data set would be on the order of 140Mb in size.

A range of statistical methodologies, including semi-blind deconvolution, image segmentation, mixture modeling, non-linear functional estimation arise in the context of the analysis of modern PET studies. This talk presents an overview of research conducted on the development of these techniques in the context of two primary applications: (i) Construction of functional images for brain and cardiac studies, and (ii), Assessment of tissue heterogeneity for human sarcoma. Data from on-going studies conducted at the University of Washington, PET imaging facility are used for illustration.

Spectral methods for noisy integral equations

Frits H. Ruymgaart (ruymg@math.ttu.edu)

Department of Mathematics and Statistics, Texas Tech University, Lubbock, USA

Inverse estimation concerns the recovery of an unknown input signal from blurred observations on a known transformation of that signal. The estimators of such indirectly observed curves to be considered here are derived from a regularized inverse of the transformation involved, exploiting Halmos's (1963) version of the spectral theorem. The usual criterion for asymptotic optimality of such curve estimators is based on the mean integrated squared error. It will be seen that the proposed estimators are rate optimal in general. One may also consider optimality related to weak convergence in the sense of Ha'jek's (1970) "convolution" theorem and its generalizations as developed in van der Vaart (1988). The curve estimators induce natural estimators for certain linear functionals that turn out to be optimal in the case of indirect density estimation. However, the estimators are not in general optimal in the indirect regression model, except when the errors are normal. This suboptimality is due to the error density that plays the role of a nuisance parameter.

Inverse problems in helioseismology

Philip B. Stark (stark@stat.berkeley.edu)

Department of Statistics, University of California, Berkeley, USA

The Sun vibrates constantly in a superposition of acoustic normal modes excited by turbulence in the Sun's convective zone. The modes have a velocity amplitude of about 1cm/s in the photosphere. They have characteristic periods on the order of 5 minutes, lifetimes ranging from hours to months, and are excited many times per lifetime. The Sun is thought to support about 10^7 modes; about 3×10^5 have been observed.

Each mode has two quantum numbers, l and m , that characterize its angular dependence, and a third quantum number, n , that characterizes its radial dependence. If the Sun were spherically symmetrical and did not rotate, the

frequencies of the $2l + 1$ modes with the same values of l and n would have the same temporal frequency; that frequency is related to soundspeed as a function of radius by an Abel transform. The Sun rotates, but not rigidly. Differential rotation splits the $2l + 1$ degenerate frequencies symmetrically. Asphericity of material properties splits the $2l + 1$ degenerate frequencies asymmetrically; this splitting is a weighted average of the rotation rate as a function of radius and latitude. The frequencies of the modes thus contain information about the composition, state, and kinematics of the solar interior. Extracting estimates of solar structure and kinematics from the normal mode frequencies are the fundamental inverse problems of normal mode helioseismology.

However, estimating the frequencies of the modes is itself an inverse problem, whose ill-posedness is exacerbated by gaps in the spatio-temporal data. Two current experiments take different approaches to reducing diurnal gaps: the SOHO project observes the Sun from orbit around the L1 Lagrange point, where the Sun never sets; the GONG network of solar telescopes spans the globe at mid latitudes, so the Sun never sets on the network. Neither experiment can observe as much as half the surface of the Sun at one time, and both suffer from occasional data loss, so there are gaps in the data.

I will present an approach to estimating solar oscillation frequencies that mitigates the problems caused by gaps by tailoring apodizing windows to the gap structure in an optimal way. The work, joint with I.K. Fodor, extends work by Thompson, Riedel, Sidorenko, Bronez and others on optimal tapering. Computing optimal tapers is very demanding computationally, but there is an inexpensive approach that is nearly optimal in practice for typical helioseismic data. The frequencies of more normal modes can be identified from these spectrum estimates than from estimates used previously by the GONG project. Calculating confidence intervals for the multitaper spectrum estimates proves to be challenging: existing methods—including parametric approximations and a variety of resampling plans in the time and frequency domains—fail, partly because of the dependence structure of the data. A novel resampling approach yields (apparently) conservative confidence intervals. Research is underway to extend the approach to estimate the spatial spectra from spherical data.

Nonparametric study of differential equations and inverse problems

Anne Vanhems (anne.vanhems@univ-tlse1.fr)

Gremaq and Crest, University Toulouse, France

The aim of our work is to provide a general framework for studying nonparametrically differential equations. We intend to replace our study in the context of inverse problems as treated by Tikhonov and Arsenin (1977) and to link it with economic issues.

Therefore, let us consider independent identically distributed observations which admit an unknown cumulative density function F . Structural econometrics considers implicit transformation of F . Of course, the theory developed depends on the nature and properties of the transformation considered. For example, there exists a wide literature about integral transformations, like additive models or instrumental variables theory. We are interested in studying differential transformations of F , and by extension of the conditional expectation. In a general way, we want to characterize the solutions of ordinary differential equations of that kind:

$$\begin{cases} y' = m(x, y, F) \\ y(x_0) = y_0 \end{cases}$$

where $y \in \mathbb{R}$ and $m : \mathbb{R} \times \mathbb{R} \times F(\mathbb{R}) \rightarrow \mathbb{R}$ is, for the moment, continuous. We want first to study the existence and unicity of a solution, that is formally to inverse a differential operator. Second, our objective is to consider the solution, if it exists, of the following system:

$$\begin{cases} y' = m(x, y, \hat{F}) \\ y(x_0) = y_0 \end{cases}$$

At last, we will study the asymptotic properties of these two solutions.

Such a purpose can be justified first by the numerous applications in economics. For example, in a microeconomic context, Hausman and Newey (1995) estimate nonparametrically the exact consumer surplus by solving a differential equation. In physics, Florens and Vanhems (2000) find the estimator of the ionosphere thickness by solving a differential equation given by physics theory. In finance, Ait-Sahalia (1996) studies the prices of derivative securities by solving a Cauchy problem.

Second, the properties of solutions of such systems are attractive. We all know that integrating a nonparametric estimator will improve its properties. More generally, we want to examine the properties of integral operators on a nonparametric estimator, and to show that it will improve it.

References

- [1] Ait-Sahalia, Y. (1993). The delta and bootstrap methods for non parametric kernel functionals. *Preprint*
- [2] Ait-Sahalia, Y. (1996). Nonparametric pricing of interest rate derivative securities. *Econometrica*, Vol.64, 527-560
- [3] Bosq, D. (1996). Non parametric statistics for stochastic processus. *Springer-Verlag*

- [4] Choquet, G. (1964). Cours d'analyse tome II Topologie. *Masson et C^{ie}*
- [5] Florens, J.P. and Vanhems, A. (2000). Nonparametric estimation of ionosphere thickness. *Preprint*
- [6] Hausman, J. and Newey, W. K. (1995). Nonparametric estimation of exact consumers surplus and deadweight loss. *Econometrica*, Vol. 63, 1445-1476
- [7] Kunze, H. E. and Vrscay, E. R. (1999). Solving inverse problems for ordinary differential equations using the Picard contraction mapping. *Inverse Problems*, Vol.15, 745-770
- [8] Sibony, M. and Mardon, J.-Cl. (1984). Approximations et equations differentielles. *Hermann*
- [9] Tikhonov, A. N. and Arsenin, V. Y. (1977). Solutions of ill-posed problems. *V.H. Winston & Sons*

Combining observations with models: Penalized likelihood and related methods in numerical weather prediction

Grace Wahba (wahba@cs.wisc.edu)

Department of Statistics, University of Wisconsin-Madison, Madison, USA

We will look at variational data assimilation as practiced by atmospheric scientists, with the eyes of a statistician. Recent operational numerical weather prediction models operate on what might be considered a very grand penalized likelihood point of view: A variational problem is set up and solved to obtain the evolving state of the atmosphere, given heterogeneous observations in time and space, a numerical model embodying the nonlinear equations of motion of the atmosphere, and various physical constraints and prior physical and historical information. The idea is to obtain a sequence of state vectors which is 'close' to the observations, close to a trajectory satisfying the equations of motion, and simultaneously respects the other information available. The state vector may be as big as 10^7 , and the observation vector 10^5 or 10^6 , leading to some interesting implementation questions. Interesting non-standard statistical issues abound.

This talk is based partly on

J. Gong, G. Wahba, D. Johnson and J. Tribbia, 'Adaptive Tuning of Numerical Weather Prediction Models: Simultaneous Estimation of Weighting, Smoothing and Physical Parameters, Monthly Weather Review 125, 210-231 (1998)

A related paper is G. Wahba, "Adaptive Tuning, four Dimensional Variational Data Assimilation, and Representers in RKHS, in 'Diagnosis of Data Assimilations Systems', Proceedings of a Workshop held at the European Centre for Medium-Range Weather Forecasts, Reading, England, March 1999, 45-52. Both are available via Grace Wahba's home page.

5 List of speakers and participants

Speakers

Robert S. Anderssen
CSIRO Mathematical and Information Sciences
GPO Box 664
Canberra, ACT 2601
Australia
E-mail: Bob.Anderssen@cmis.csiro.au

Jose M. Angulo
Department of Statistics and Operations Research
Faculty of Sciences
University of Granada
Campus Fuente Nueva s/n
Spain
E-mail: jmangulo@ugr.es

Viktor Benes
Department of Probability and Statistics
Charles University
Faculty of Mathematics and Physics
Sokolovska 83
18675 Praha 8
The Czech Republic
E-mail: benesv@karlin.mff.cuni.cz

Per Christian Hansen
Informatics and Mathematical Modelling
Technical University of Denmark
Richard Petersens Plads
Building 321
2800 Kongens Lyngby
Denmark
E-mail: pch@imm.dtu.dk

Marcela Hlawiczkova
Department of Probability and Statistics Charles University
Faculty of Mathematics and Physics
Sokolovska 83
18675 Praha 8
The Czech Republic
E-mail: mhlawiczkova@yahoo.com

Markus Kiderlen
Mathemat. Inst. II
University of Karlsruhe
76128 Karlsruhe
Germany
E-mail: kiderlen@imf.au.dk

Odd Kolbjørnsen
Department of Mathematical Sciences
Norwegian University of Science and Technology
7491 Trondheim
Norway
E-mail: ok@math.ntnu.no

Robin Morris
USRA-RIACS
NASA Ames Research Center, Mail Stop 269-2
Moffett Field, CA 94035-1000
USA
E-mail: rdm@ptolemy.arc.nasa.gov

Klaus Mosegaard
Department of Geophysics
University of Copenhagen
Juliane Maries Vej 30
2100 Copenhagen Ø
Denmark
E-mail: klaus@gfy.ku.dk

Geoff Nicholls
Department of Mathematics
University of Auckland
Private Bag 92019
Auckland
New Zealand
nicholls@math.auckland.ac.nz

Doug W. Nychka
Geophysical Statistics Project
National Center for Atmospheric Research
Climate and Global Dynamics Division
Boulder, CO 80302
USA
E-mail: nychka@cgd.ucar.edu

Henning Omre
Department of Mathematical Sciences
Norwegian University of Science and Technology
7491 Trondheim
Norway
E-mail: omre@math.ntnu.no

Finbarr O' Sullivan
Department of Statistics
University College Cork
Cork
Ireland
E-mail: finbarr@stat.ucc.ie

Maria D. Ruiz-Medina
Department of Statistics and Operations Research
Faculty of Sciences
University of Granada
Campus Fuente Nueva s/n
Spain
E-mail: mruiz@ugr.es

Frits H. Ruymgaart
Department of Mathematics and Statistics
Texas Tech University
Box 41042
Lubbock, TX 79409-1042
USA
ruymg@math.ttu.edu

Philip B. Stark
Department of Statistics
University of California
Berkeley, CA 94720-3860
USA
E-mail: stark@stat.Berkeley.EDU

Anne Vanhems
Gremaq - Universit des Sciences Sociales
Manufacture des Tabacs
21, allés de Brienne
31000 Toulouse
France
E-mail: anne.vanhems@univ.tlse1.fr

Grace Wahba
Department of Statistics
University of Wisconsin-Madison
1210 West Dayton Street
Madison, WI 53706-1685
USA
wahba@stat.wisc.edu

Participants

Kim Emil Andersen
Department of Mathematical Sciences
Aalborg University
Fredrik Bajers Vej 7G
9220 Aalborg Ø
Denmark
E-mail: emil@math.auc.dk

Marie Lund Andersen
Informatics and Mathematical Modelling
Technical University of Denmark
Richard Petersens Plads
Building 305
2800 Kongens Lyngby
Denmark
E-mail: marie915@forum.dk

Ann-Charlotte Berglund
Informatics and Mathematical Modelling
Technical University of Denmark
Richard Petersens Plads
Building 321
2800 Kongens Lyngby
Denmark
E-mail: acb@imm.dtu.dk

Svend Berntsen
Department of Mathematical Sciences
Aalborg University
Fredrik Bajers Vej 7G
9220 Aalborg Ø
Denmark
E-mail: sb@math.auc.dk

Kasper Berthelsen
Department of Mathematical Sciences
Aalborg University
Fredrik Bajers Vej 7G
9220 Aalborg Ø
Denmark
E-mail: kkb@math.auc.dk

Ole F. Christensen
Department of Mathematical Sciences
Aalborg University
Fredrik Bajers Vej 7G
9220 Aalborg Ø
Denmark
E-mail: olefc@math.auc.dk

Horia Cornean
Department of Mathematical Sciences
Aalborg University
Fredrik Bajers Vej 7G
9220 Aalborg Ø
Denmark
E-mail: cornean@math.auc.dk

Martin B. Hansen
Department of Mathematical Sciences
Aalborg University
Fredrik Bajers Vej 7G
9220 Aalborg Ø
Denmark
E-mail: mbh@math.auc.dk

Sture Holm
Matematisk Statistik
Chalmers
SE-41296 Göteborg
Sweden
E-mail: holm@math.chalmers.se

Michael Jacobsen
Informatics and Mathematical Modelling
Technical University of Denmark
Richard Petersens Plads
Building 305
2800 Kongens Lyngby
Denmark
E-mail: mj@imm.dtu.dk

Jens Ledet Jensen
Department of Mathematical Sciences
Theoretical Statistics
University of Aarhus
8000 Aarhus C
Denmark
E-mail: jlj@imf.au.dk

Jon Johnsen
Department of Mathematical Sciences
Aalborg University
Fredrik Bajers Vej 7G
9220 Aalborg Ø
Denmark
E-mail: jjohnsen@math.auc.dk

Rikke Høj Kjeldsen
Informatics and Mathematical Modelling
Technical University of Denmark
Richard Petersens Plads
Building 305
2800 Kongens Lyngby
Denmark
E-mail: rikke@ostenfeld.dk

Kim Knudsen
Department of Mathematical Sciences
Aalborg University
Fredrik Bajers Vej 7G
9220 Aalborg Ø
Denmark
E-mail: kim@math.auc.dk

Steffen L. Lauritzen
Department of Mathematical Sciences
Aalborg University
Fredrik Bajers Vej 7G
9220 Aalborg Ø
Denmark
E-mail: steffen@math.auc.dk

Roderik V.N. Melnik
University of Southern Denmark
Mads Clausen Institute
Grundtvigs Alle 150
6400 Sønderborg
Denmark
E-mail: rmelnik@mci.sdu.dk

Jesper Møller
Department of Mathematical Sciences
Aalborg University
Fredrik Bajers Vej 7G
9220 Aalborg Ø
Denmark
E-mail: jm@math.auc.dk

Steen Møller
Department of Mathematical Sciences
Aalborg University
Fredrik Bajers Vej 7G
9220 Aalborg Ø
Denmark
E-mail: moeller@math.auc.dk

Anders Nielsen
Department of Mathematics and Physics
The Royal Veterinary and Agricultural University
Thorvaldsensvej 40
1871 Frederiksberg C
Denmark
E-mail: an@dfu.min.dk

Jonny Olsson
Statistical Norm
Bomvägen 20
226-51 Lund
Sweden
E-mail: jonny.olsson@mailbox.swipnet.se

Frede Tøgersen
Biometry Research Unit
Department of Agricultural Systems
Research Centre Foulum
P.O. Box 50
8830 Tjele
Denmark
E-mail: FredeA.Togersen@agrsci.dk

Samuli Siltanen
Instrumentarium Corp. Imaging Division
P.O. Box 20
04301 Tuusula
Finland
E-mail: samuli.siltanen@fi.instrumentarium.com

Christian Bressen Pipper
Department of Mathematics and Physics
The Royal Veterinary and Agricultural University
Thorvaldsensvej 40
1871 Frederiksberg C
Denmark
E-mail: bressen@dina.kvl.dk

Jan Marthedal Rasmussen
Informatics and Mathematical Modelling
Technical University of Denmark
Richard Petersens Plads
Building 305
2800 Kongens Lyngby
Denmark
E-mail: jmr@imm.dtu.dk

Christian Ritz
Department of Mathematics and Physics
The Royal Veterinary and Agricultural University
Thorvaldsensvej 40
1871 Frederiksberg C
Denmark
E-mail: ritz@dina.kvl.dk